

# Measurements of Elastic Scattering and Total Non-Elastic Cross Sections for 40-80 MeV Neutrons at TIARA

Masanobu IBARAKI<sup>(1)</sup>, Hiroshi NAKASHIMA<sup>(2)</sup>, Shin-ichiro MEIGO<sup>(2)</sup>,  
Mamoru BABA<sup>(1)</sup>, Takako MIURA<sup>(1)</sup>, Yoshitaka HIRASAWA<sup>(1)</sup>,  
Tsutomu HIROISHI<sup>(1)</sup>, Takao AOKI<sup>(1)</sup>, Susumu TANAKA<sup>(3)</sup>

*E-mail: iba@rpl.qse.tohoku.ac.jp*

*(1)Department of Quantum Science and Energy Engineering, Tohoku University, Sendai 980-8579*

*(2)Tokai Establishment, Japan Atomic Energy Research Institute, Tokai-Mura 319-11*

*(3)Takasaki Establishment, Japan Atomic Energy Research Institute, Takasaki 370-123*

We have performed the measurements of neutron elastic scattering and total non-elastic cross sections of carbon, silicon, iron, zirconium and lead in 40-80 MeV region using a  ${}^7\text{Li}(p,n)$  quasi-monoenergetic neutron source at TIARA of JAERI. Elastic scattering cross sections for 55, 65 and 75 MeV neutrons were measured by time-of-flight method at 25 laboratory angles between  $2.6^\circ$  and  $53.0^\circ$ . Total non-elastic cross sections for 40-80 MeV neutrons were measured by attenuation methods. The experimental data were compared with the other experimental data and the libraries.

## 1 Introduction

Neutron cross section data above 20 MeV become more and more important for the shielding design of the high-energy accelerator facilities, estimation of radiation damage and for various applications. Total, elastic scattering and non-elastic cross section data with appropriate accuracy are required for the evaluation of intermediate nuclear data. However, experimental data of elastic scattering and non-elastic cross section are very scarce above 40 MeV because of the experimental difficulties, in contrast to the total cross section data for which very accurate data are available[1, 2].

In this study, we have performed measurements of elastic scattering and non-elastic cross section for carbon, silicon, iron, zirconium and lead in 40-80 MeV region at TIARA facility of JAERI[3]. Elastic scattering cross sections were measured by the time-of-flight (TOF) method at 25 laboratory angles between  $2.6^\circ$  and  $53.0^\circ$  with five liquid scintillator detectors. Total non-elastic cross sections were measured by the attenuation method adopting a “close-geometry”[4, 5] and a large plastic scintillator detector. The experimental results were compared with the other experimental data and libraries.

## 2 Elastic Scattering Measurements

### 2.1 Experiment and data reduction

Measurements were done at 75, 65 and 55 MeV by using the time-of-flight (TOF) method and the  ${}^7\text{Li}(p,n)$  quasi-monoenergetic neutron source [3]. The details of experimental and data reduction method is described elsewhere[6, 7]. Data were obtained for carbon, silicon, iron, zirconium and lead at 25 laboratory angles between  $2.6^\circ$  and  $53.0^\circ$ . The effects of inelastically scattered neutrons were corrected by calculating the fraction of the inelastic neutrons to the total (sum of the elastic and inelastic) ones considering experimental energy resolution using the LA 150 data [8].

## 2.2 Results

Figure 1 shows the results of carbon, iron and lead in comparison with the data reported by the U.C.Davis group[9, 10]. They measured neutron elastic scattering cross sections for 65 MeV by a  ${}^7\text{Li}(p,n)$  source and 52.5-225 MeV by a spallation neutron source. By adopting the TOF method with a longer flight path at TIARA facility, our data cover much wider angular range than that of Davis ones. In comparison of 65 MeV data, the Davis's data for iron around  $25^\circ$  differ from the present one by about 40%, while they are in good agreement for other elements. The Davis's data by spallation source were restricted to angular range of  $7^\circ$ - $23^\circ$ , and show milder distribution than our results.

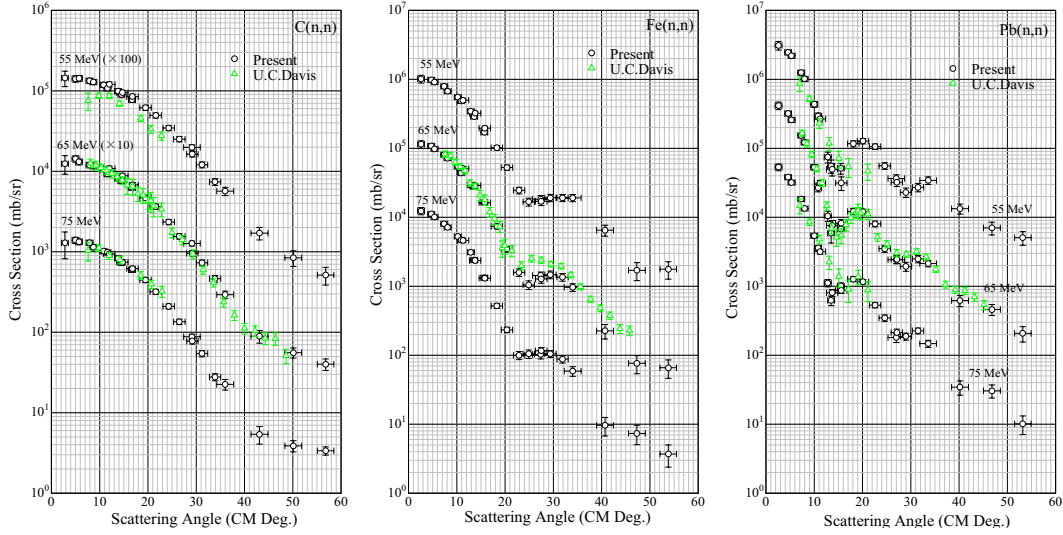


Figure 1: Elastic scattering cross sections of C(n,n), Fe(n,n) and Pb(n,n) in comparison with U.C.Davis data

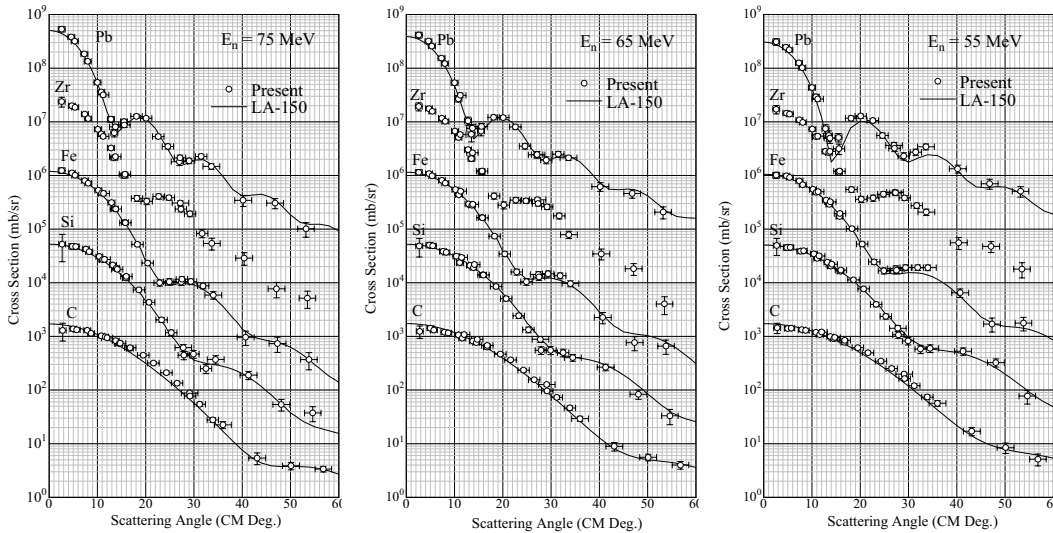


Figure 2: Elastic scattering cross sections in comparison with LA 150

Figure 2 shows the present result in comparison with the LA 150 data[8]. LA 150 is the evaluated neutron and proton cross section library up to 150 MeV. The neutron optical potentials by A.S.Meigooni et al.[11] for carbon, D.G.Madland[12] for silicon and iron, R.E.Shamu and P.G.Young[13] for lead, are used, in this energy region. In general, LA150 data agree well with the present results for all nuclei and incident energies, but in detail, are smaller by 10-15% for Pb at forward angles.

Figure 3 shows angle-integrated elastic scattering cross sections in comparison with the LA150 data, Pearlstein’s systematics[14] and other experimental data. The present angle integrated cross sections were deduced by least-square fitting of optical model calculation using a code, *ECIS88*, to each differential cross section. LA 150 data agree well present data except for lead,  $\sim 10\%$  smaller.

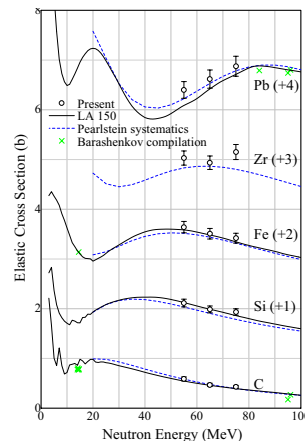


Figure 3: Angle integrated elastic scattering cross sections

### 3 Total Non-elastic Measurements

#### 3.1 Experiment and data reduction

Neutron total non-elastic cross sections of carbon, silicon, iron, zirconium and lead were measured in 40-80 MeV region based on the attenuation method adopting with “close-geometry” [4, 5]. Figure 4 shows the setup of the total non-elastic measurements. In this method, the neutron detector subtends large solid angle to the sample, and detects both the transmitted neutrons which did not receive any reaction in the sample and most of the elastically scattered neutrons by the sample. The total non-elastic cross section was deduced by following equation while some corrections are needed,

$$\sigma_{ne} \approx -\ln(I_m/I_0)/(Nt), \quad (1)$$

where  $I_0$  is the incident neutron flux measured by the sample-out run,  $I_m$  is the neutron flux transmitted through the sample measured by the sample-in run. The thickness of the samples,  $t$ ,  $3\sim 4$ cm, was chosen so that  $\exp(-\sigma_{ne}Nt) = 0.8 \sim 0.9$ . The neutron beam was collimated to 1 cm diam. by iron so that the beam spot was smaller than the diameter of the samples, 2 cm. The transmissions,  $I_m/I_0$ , were obtained concurrently for 40-80 MeV neutrons by using a peak and continuous part of the  ${}^7\text{Li}(p,n)$  neutron source with  $E_p=80$  MeV [3]. We used an NE 102 plastic scintillator,  $20.3\text{cm} \phi \times 7.6\text{cm}$ , located at 12 cm or 18 cm from the sample. The detector subtending a large angle,  $\theta_{max}=30\sim 40^\circ$ , intercepted most of the elastically scattered neutrons, 95% typically. Table 1 shows the structure of the energy bin and the detector threshold energy. The threshold for each incident neutron energy was selected as a compromise between the detector efficiency and the effects of inelastically scattered neutrons.

Table 1: Structure of the energy group and detector threshold

| $E_n$ (MeV)        | 75        | 65        | 60        | 55        | 50        | 45        |
|--------------------|-----------|-----------|-----------|-----------|-----------|-----------|
| $\Delta E_n$ (MeV) | 72.5-78.5 | 62.5-67.5 | 57.5-62.5 | 52.5-57.5 | 47.5-52.5 | 42.5-47.5 |
| Bias(MeV)          | 50        | 40        | 30        | 30        | 20        | 20        |

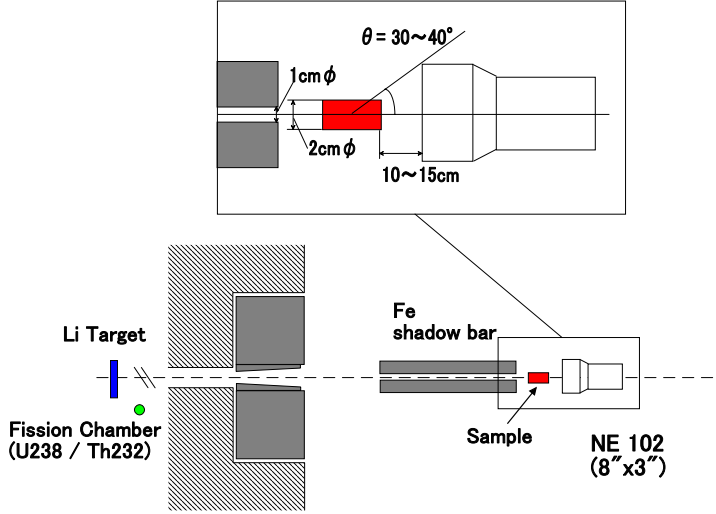


Figure 4: Experimental set up of total non-elastic cross section measurement

Figure 5 shows the attenuated (sample-in, iron) and direct (sample-out) TOF spectra. The  $I_m$  and  $I_0$  for each energy group were deduced by integrating over the corresponding ROI in TOF spectra. To deduce total non-elastic cross section, the corrections were considered for the probabilities of 1) the neutrons elastically scattered to the angles larger than  $\theta_{max}$ ,  $f_1 = \frac{1}{\sigma_{el}} \int_{\theta_{max}}^{\pi} d\Omega \frac{d\sigma_{el}}{d\Omega}$ , 2) the neutrons inelastically scattered to the angles smaller than  $\theta_{max}$ ,  $f_2 = \frac{1}{\sigma_{ne}} \int_{E_b}^{E_{in}} dE \int_0^{\theta_{max}} d\Omega \frac{d^2\sigma_{ne}}{d\Omega dE}$ , where  $E_b$  is detector threshold energy and 3) the neutrons elastically scattered to the angles smaller than  $\theta_{max}$  are not detected because of multiple-scattering,  $f_3 = \frac{1}{\sigma_{el}} \int_0^{\theta_{max}} d\Omega \frac{d\sigma_{el}}{d\Omega} (1 - e^{-\sigma_t N \bar{x}}) \frac{\sigma_{ne}}{\sigma_t}$ , where  $\bar{x}$  is mean path length in the sample. To calculate  $f_{1,2,3}$ , we used the experimental data[1, 2] for total cross section and the LA 150 data[8] for the angular distribution of elastic scattering. The experimental total cross sections have relatively small uncertainties, 1% or smaller, and the elastic scattering cross sections of LA 150 reproduce the experimental data as seen in Fig.2. Because  $f_3$  explicitly includes the  $\sigma_{ne}$  we want, we made iterative calculations to find a solution. Typically,  $f_1$ ,  $f_2$  and  $f_3$  were respectively 2%~10%, 4%~8% and 4%~10% but depend on the neutron energy and sample. The corrected cross section was deduced by the following equations.

$$\frac{I_m}{I_0} = e^{-\sigma_t N t} + (1 - e^{-\sigma_t N t}) \frac{1}{\sigma_t} ((1 - f_1 - f_3) \sigma_{el} + f_2 \sigma_{ne}), \quad (2)$$

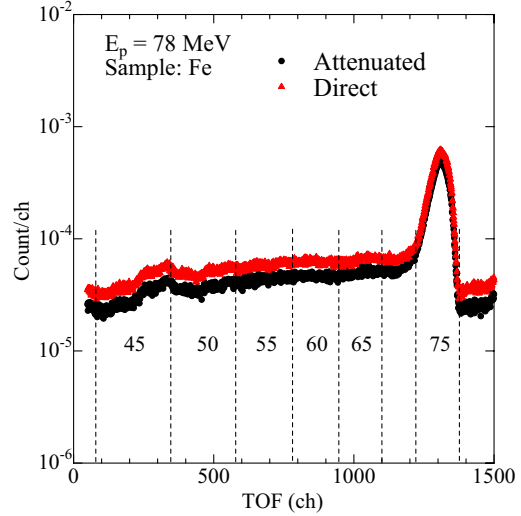


Figure 5: Attenuated (sample-in) and direct (sample-out) TOF spectra

then we substitute  $\sigma_t - \sigma_{ne}$  to  $\sigma_{el}$ ,

$$\sigma_{ne} = \frac{\frac{I_m - 1}{I_0} + f_1 + f_3}{f_1 + f_2 + f_3 - 1} \sigma_t \quad (3)$$

where  $\sigma_t$  is experimental total cross section[1, 2]. Figure 6 shows the comparison with raw and corrected total non-elastic cross sections. The differences between corrected and uncorrected data are 5% to 15%.

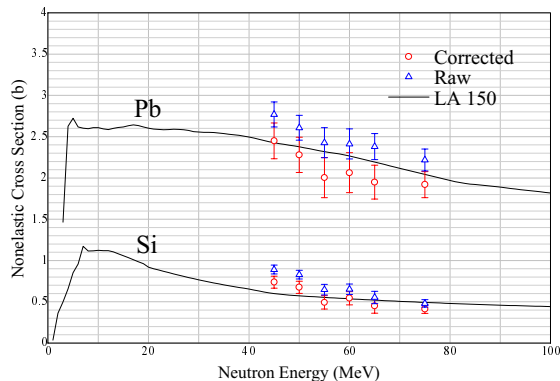


Figure 6: Comparison with raw and corrected total non-elastic cross sections

### 3.2 Results

Figure 7 shows the present results in comparison with other experimental data, Pearlstein’s systematics[14] and LA 150 data. The circles are deduced from the present (n,n) data by subtracting the present elastic scattering cross section from well-known total cross section[1, 2]. The data by our two experiments agree each other with experimental uncertainties except for zirconium at 75 MeV. The present experiment provide the data at 40-80 MeV region where there were only few experiments, and are useful to verify the calculations. Above 50 MeV, our results supports the LA 150 data and systematics except for lead case. For lead, the present results are close to systematics rather than the LA 150 data which are larger by 15% in 50-80 MeV region. Figure 8 shows the present results for lead in comparison with proton data as well as neutron one. The present results are close to proton data by LA 150 and experiments, and neutron total-nonelastic cross sections by LA 150 seem to be too large.

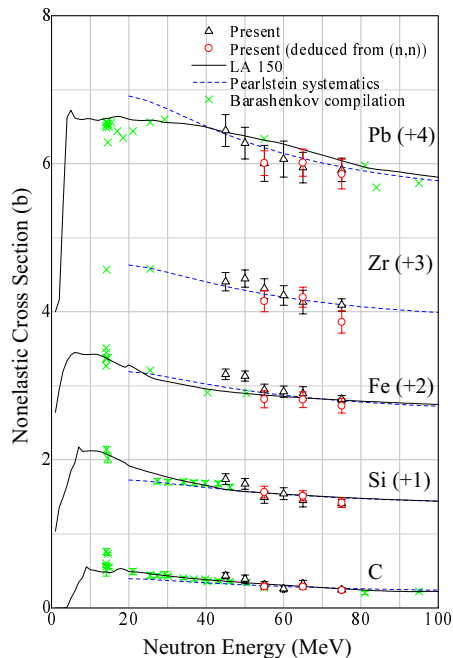


Figure 7: Total non-elastic cross section

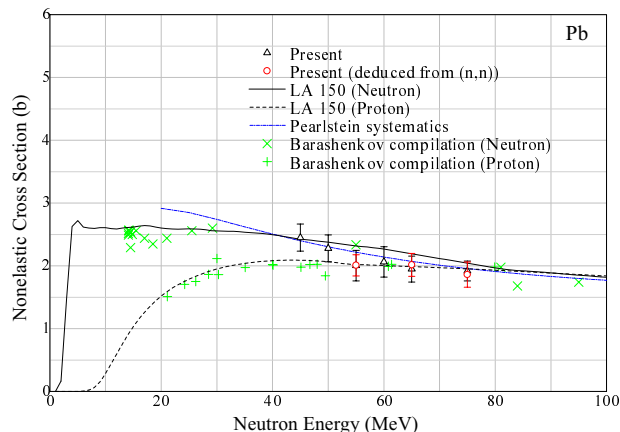


Figure 8: Total non-elastic cross sections for lead

## 4 Summary

Neutron elastic and total non-elastic cross sections were measured in 40-80 MeV region by TOF and attenuation methods, respectively. Elastic scattering measurements were done for 75, 65 and 55 MeV neutrons, and the data at 25 laboratory angle points between  $2.6^\circ$  and  $53.0^\circ$  were obtained. LA 150 reproduced the elastic scattering cross sections very well except for lead at very forward angles. The total non-elastic cross sections by two experiments were consistent within experimental uncertainties. LA 150 data reproduced experiments very well except for lead,  $\sim 15\%$  larger of total non-elastic cross sections.

## References

- [1] R.W.Finlay et al., Phys. Rev. C 47 (1993) 237
- [2] F.S.Dietrich et al., Proc. Int. Conf. on Nuclear Data for Sci. and Technol, 1997 Trieste, (1998) p.402
- [3] M.Baba et al., Nucl. Instrum. and Methods A 428 (1999) 454
- [4] R.G.P.Voss and R.Willson, Proc. Phil. Soc. (London), A 236 (1956) 41
- [5] F.P.Brady et al., Nucl. Instrum. and Methods, 178 (1980) 427
- [6] M.Ibaraki et al., Nucl. Instrum. and Methods A, to be published.
- [7] M.Ibaraki et al., Proc. Ninth International Conf.on Rad. Shielding (ICRS9), 1999 Tsukuba, to be published.
- [8] M.B.Chadwick et al., Nucl. Sci. Eng. 131, (1999) 293
- [9] E.L.Jort et al., Phys. Rev. C 53 (1996) 237
- [10] J.H.Osborn, Dissertation, University of California, Davis (1995)
- [11] A.S.Meigooni et al., Nucl. Phys. A, 445 (1985) 305
- [12] D.G.Madland, Proc. OECD/NEANDC Specialist's Mtg. on Preeq. Nucl. Reac., 1988 Semmering, NEANDC-245 (1988)
- [13] R.E.Shamu and P.G.Young, J. Phys. G 19 (1993) L169
- [14] S.Pearlstein, Astrophys. Journal, 346 (1989) 1049